



Evaluation of artificial neural network and Penman–Monteith equation for the prediction of barley standard evapotranspiration in a semi-arid region

Masoumeh Hashemi¹ · Ali Reza Sepaskhah¹

Received: 28 March 2018 / Accepted: 1 August 2019 / Published online: 17 August 2019
© Springer-Verlag GmbH Austria, part of Springer Nature 2019

Abstract

Evapotranspiration (ET) is a main factor of the hydrologic balance. Estimating precise ET is necessary for managing the water supply in a basin. In this study, daily barley standard evapotranspiration (DBSE) is obtained (1) directly by weighing lysimeter and (2) indirect methods. In the first step, DBSE was obtained by two weighing lysimeters in a semi-arid region (Kooshkak, Iran). In the next step, indirect methods for estimating the DBSE, the Penman–Monteith (PM), and the artificial neural networks (ANNs), including the radial basis functions (RBF), and the multi-layer perceptron (MLP), were utilized. Results showed that DBSE can be successfully calculated in semi-arid region by MLP-ANN, RBF-ANN, and PM methods. The ANN methods were offered as the best method because they need fewer input data and can be easily used for other developed programs that applied for water allocation and therefore solve the conflicts between stakeholders and optimize water usage. Finally, the sensitivity of ANNs to input data was investigated by relating changes in the daily metrological data to the dimensionless scaled sensitivities (DSS) index. Results showed that in the multi-layer perceptron, ET_c was more sensitive to sunshine hours and less sensitive to wind speed and the radial basic function has different patterns which are more sensitive to sunshine hours. When the sunshine hours decrease by more than 10%, the standard crop evapotranspiration (ET_c) was more sensitive to average humidity and less sensitive to wind speed.

1 Introduction

In recent decades, water resources have gradually decreased in a semi-arid region of Iran mainly due to a decrease in seasonal precipitation and an increase in both water demand and temperature. Obviously, water availability is one of the most important factors for crop production in the arid and semi-arid regions. Therefore, a careful understanding of the water balance is important in determining water-saving measures (Li et al. 2003). Crop evapotranspiration is one of the most important parameters of water balance and is a major factor in the optimal irrigation schedule to improve water use efficiency in the irrigated land (Li et al. 2003). This study is the first report

that presented DBSE and offered an optimal indirect method for calculating DBSE in semi-arid climates.

Crop evapotranspiration is directly calculated by measurement of soil water loss, or by indirect methods such as the aerodynamic method, the energy balance method, and the combination of them. The direct method is costly and time-consuming (Falamarzi et al. 2014); therefore, the indirect methods are more commonly used. Most of the prevalent models for predicting ET_c are the physically based or empirical equations that were developed based on climatological variables (Sudheer et al. 2003).

The Penman–Monteith (FAO-PM56) as a standard indirect method has been recommended for use by the Food and Agriculture Organization (FAO) (Allen et al. 1998) and therefore, FAO-PM56 is the most prevalent method used. However, the FAO-PM56 approach needs a large amount of climatic data; for this reason, simpler methods were developed that require less meteorological variables (Kumar et al. 2008; Moghaddamnia et al. 2009; Traore et al. 2010; Amba and Baltas 2012; Ladlani et al. 2012; Aghajani et al. 2012; Shahrokhnia and Sepaskhah 2013; Abrishami-Shirazi et al. 2019; Kisi 2010).

✉ Ali Reza Sepaskhah
sepas@shirazu.ac.ir

Masoumeh Hashemi
m.hashemitame@edu.ikiu.ac.ir

¹ Irrigation Department, Shiraz University, Shiraz, I.R. of Iran

Crop evapotranspiration is a nonlinear and complex phenomenon; its design depends on the number and types of meteorological data obtained and their impact on each other (Landeras et al. 2008). In recent decades, notable advances in the field of nonlinear-pattern identification have been made to a branch of the nonlinear theoretical system of modeling that is called artificial neural network (ANN). The ANN is a nonlinear mathematical structure capable of identifying arbitrarily complex nonlinear processes that map the input and output of any system (Sudheer et al. 2003).

Sudheer et al. (2003) used radial basis function (RBF)-ANNs to evaluate daily ET_c for rice crops. The crop evapotranspiration was simulated using the RBF-ANN model and was compared with the lysimetric data. The results clearly showed the proficiency of the ANN method in calculating the ET_c . Trajkovic (2005) investigated the reference potential evapotranspiration (ET_o) using Hargreaves and Thornthwaite methods in Serbia from which a radial basis function (RBF) network was also used to compute ET_o using temperature data. The result showed that RBF has a higher performance in ET_o estimation than the two other methods. Zanetti et al. (2007) used the artificial neural networks for estimating the ET_o by using only data from the maximum and minimum air temperatures. The multi-layer perceptron networks showed the best results when composed of a single hidden layer with ten neurons and hyperbolic tangent sigmoid-type activation function. Dehbozorgi and Sepaskhah (2012) employed the Penman-FAO (P-FAO), Penman-Monteith, empirical model, and artificial neural network to estimate the reference potential evapotranspiration in the semi-arid region. The ANNs with six inputs had better performance than the P-FAO equation and were similar to the PM equation. In addition, the prediction performance of ANNs, with four input parameters, was higher than the PM equation and was similar to P-FAO and the developed empirical equations. Abrishami et al. (2019) utilized ANN-MLP to estimate the daily ET_c of wheat and maize in a semi-arid region. These networks, which used climatic data, leaf area index, and plant height for both crops, demonstrated the proficiency of MLP-ANN method with two hidden layers in the estimation of daily ET_c . Kisi and Kilic (2015) estimated the ability of ANNs and M5 model tree (M5Tree) in modeling ET_o . It was found that the ANN had better performance than the PM and Turc methods in estimation of the ET_o .

Global warming and climate change are anticipated to affect the climatic parameters to varying degrees which, in turn, affect the evapotranspiration. Therefore, it is important to determine which meteorological variable has a higher effect on ET_c . Sensitivity analysis can assess the sensitivity of model output with respect to variation in the model parameters (Saltelli et al. 2004). Sensitivity analysis plays an important

role in understanding the connection between climate data availability and prediction precision of ET_o and between the climatic condition and ET_o variation (Gong et al. 2006). In addition, the sensitivity of the input data for evapotranspiration models is applied to find the best input data and determine the most effective parameters in evapotranspiration. Many investigations have studied the sensitivity of different variables for the ET_c and ET_o estimation methods (Beven 1979; Ambas and Baltas 2012; Sharifi and Dinpazhoh 2014).

Cereals are the most important food crops and have provided 70 percent of the food for the world's population. Of these, barley is the world's fourth most important cereal and an important livestock feed product in Iran. For this reason, it is used as the test crop in this study.

The aims of this study include (1) mensuration of barley evapotranspiration by weight lysimeters in an area in the semi-arid climate of Kooshkak, (2) calculation of DBSE by Penman-Monteith equation and artificial neural networks (indirect methods), (3) comparison between the indirect methods with the measured data and (4) investigation of the sensitivity of the input data for the indirect methods.

2 Materials and methods

2.1 Study area

The study area is Kooshkak Agricultural Research Station (Faculty of Agriculture, Shiraz University), located in Fars Province in the southwest of Iran at latitude $30^{\circ} 4' 45''$, longitude $52^{\circ} 35' 14''$ and 1620 m above mean sea level (Fig. 1). The long-term mean climate parameters of the research station are annual precipitation 412 mm, wind velocity 0.75 m s^{-1} , relative humidity 50.5%, wind velocity 0.75 m s^{-1} , air temperature 15.68°C , daily pan evaporation 5.8 mm, and daily sunshine 8.4 h (Shahrokhnia and Sepaskhah 2012). The regional climate is classified as semi-arid (Malek 1982).

2.2 A direct method of measuring evapotranspiration

Barley (*Hordeum vulgare*) was planted in two large-scale weighing lysimeters with each area of 7.07 m^2 . The lysimeters are installed in the middle of a field with an area of 1600 m^2 . The same cultivation practices were used in both the lysimeter sites and their surrounding field and they were irrigated with the same frequency and amount.

The leaf area index (LAI) and crop height were recorded at 7-day interval. During the growing season, the crops were irrigated using furrow irrigation with well water. Crops in the lysimeters and surrounding field were protected from disease, pests, and water stress which are the standard conditions

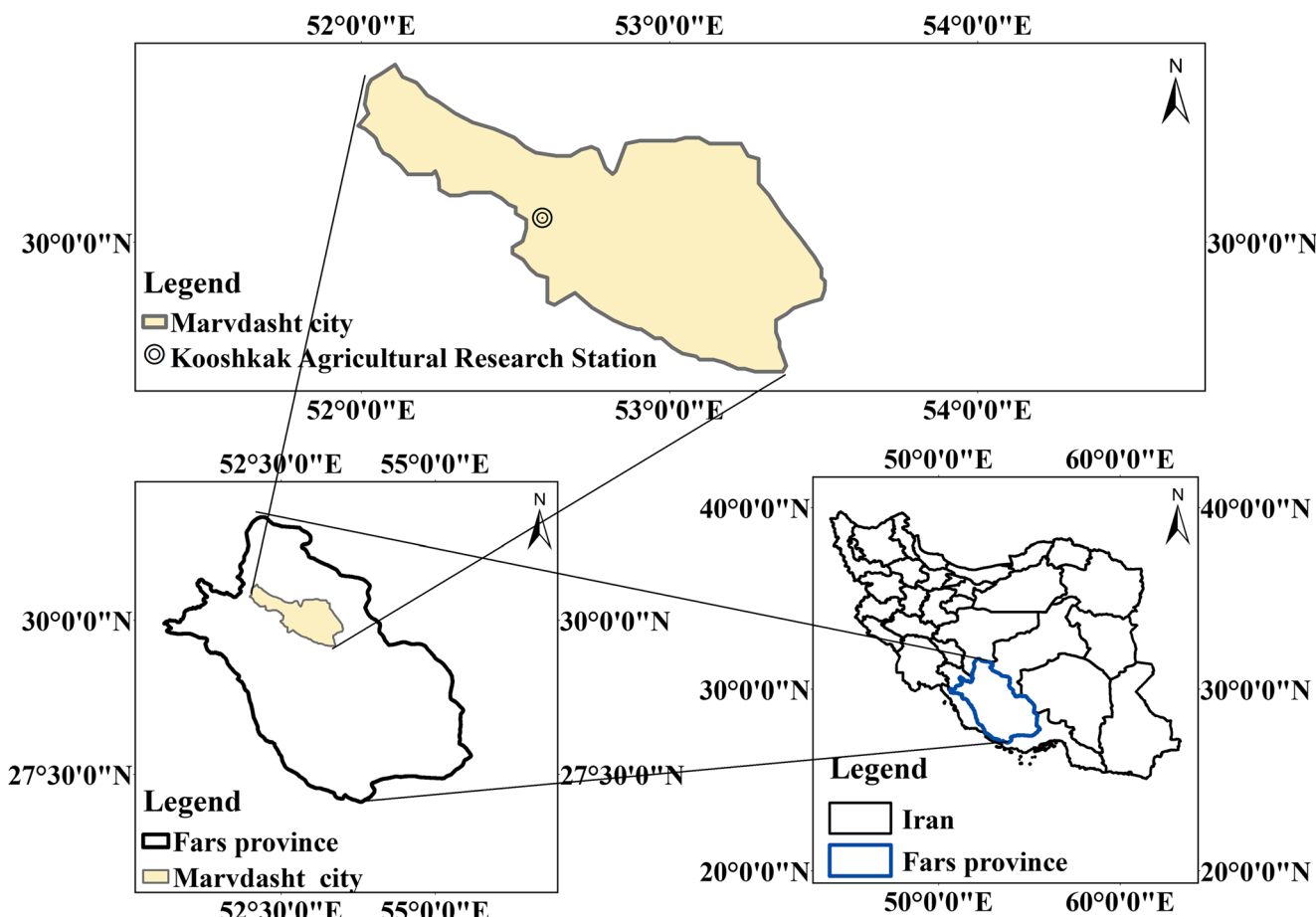


Fig. 1 Map of the research station located in Marvdasht city, Iran

for the daily barley evapotranspiration (ET_c). Daily ET_c values in two lysimeters were determined by using the difference between weights of lysimeters based on precipitation, irrigation, and deep percolation amounts in a 24-h period from 21 November 2011 to 12 June 2012. The DBSE was determined based on the water balance principle as follows:

$$ET_c = P + I - D + \Delta w \tag{1}$$

where ET_c is the standard crop evapotranspiration ($\text{mm}^3 \text{ day}^{-1}$), P is the precipitation (mm^3), I is the amount of irrigation (mm^3), D is the deep percolation (mm^3), and Δw is the daily change in weight of the lysimeters (equivalent mm^3). Details of measurement procedure were reported by Hashemi (2013).

2.3 Penman–Monteith equation (indirect method)

In 1948, Penman developed the mass transfer procedure and the energy balance and derived an equation accordingly. This equation calculated the evaporation from an open water surface by using standard climatological parameters such as sunshine, wind speed, humidity, and temperature. The combination equation was developed later by many researchers. They

extended the equation to cropped surfaces by considering resistance factors. The Penman–Monteith equation for computing ET_c is as follows:

$$ET_c = \frac{\Delta(Rn - G) + \rho c_p \left\{ \frac{e_s - e_a}{r_a} \right\}}{\lambda \left(\Delta + \gamma \left\{ 1 + \frac{r_s}{r_a} \right\} \right)} \tag{2}$$

where ET_c is the crop evapotranspiration rate at standard conditions ($\text{mm} \cdot \text{d}^{-1}$), Rn is the solar radiation ($\text{MJ m}^{-2} \cdot \text{d}^{-1}$), G is the soil heat flux ($\text{MJ m}^{-2} \cdot \text{d}^{-1}$), c_p is the specific heat of moist air ($\text{kJ kg}^{-1} \text{ }^\circ\text{C}^{-1}$), Δ is the slope of the saturation pressure versus temperature function ($\text{kPa }^\circ\text{C}^{-1}$), ρ is the air density (kg m^{-3}), γ is the psychrometric constant ($\text{kPa }^\circ\text{C}^{-1}$), $(e_s - e_a)$ is the vapor pressure deficit of the air (kPa), r_s and r_a are the (bulk) surface and aerodynamic resistance (s m^{-1}), and λ is the latent heat of evaporation (MJ kg^{-1}). The calculated daily value of G is very small so it is considered as zero in the computation.

The aerodynamic resistance and the (bulk) surface are important components of Penman–Monteith equations presented in the FAO56 (Allen et al. 1998). The equations depend on the height and leaf area of barley as measured in the field.

2.4 Artificial neural network (indirect method)

ET_c is a complex and nonlinear process which depends on the interacting climatology factors and their indigenous features. However, the lack of physical understanding of the ET_c procedure and unavailability of relevant data results in imprecise calculations of the ET_c. Over the past two decades, artificial neural networks (ANNs) have been increasingly used in modeling of hydrological processes because of their high ability to simulate hydrologic variables without any understanding of physical processes (Kumar et al. 2011; Abrishami et al. 2019; Dehbozorgi and Sepaskhah 2012).

In this study, for ANN model, daily average temperature (°C), daily average humid (%), daily wind speed (m s⁻¹), and daily sunshine hours (h) were used as input data and the measured DBSE as output data. All the input data were randomly divided into training and testing subsets as follows: three-quarters of the data for the training set and a quarter of the data for the testing set. The training data set was used for calculating the gradient and updating the network biases and weights, whereas, the testing data set was used for validating the network performance. To attain the best artificial neural network, two neural networks, radial basis function (RBF) and multi-layer perceptron (MLP), were evaluated.

2.4.1 Radial basis functions

The radial basis function network is a network that applies radial basis functions as the transfer functions for finding features of input data. Radial basis functions of the outputs and nodes parameters are a linear combination of the output of the RBF.

The radial basis function (RBF) networks have three layers: an input layer, a feature layer with a radial basis transfer function, and a linear output layer (Fig. 2).

The input data is defined as a vector that is a set of real numbers $x \in R^n$. The output data of the feature layer is modeled as a vector function of the center vector and input vector and $H_j(x) : R^n \rightarrow R^m$ is shown as follows:

$$H_j(x) = \rho(\|x - c_j\|) \tag{3}$$

where c_j is the center vector for center j of the feature layer and ρ is the radial function. The function depends only on the distance between each center vector and input vector, accordingly entitled radial basis function. The Euclidean distance and Gaussian function as base function normally are used for radial basis function network. The equation for the calculation is:

$$y = \sum_{j=1}^m w_j H_j(x) + w_0 \tag{4}$$

where w_j is the weight of the j th center to the neuron of the output, w_0 is the bias of the neuron of the output, m is the number of feature layer neurons, and y is the amount of output.

The parameters w_j , w_0 , m , and c_j are computed in an approach that optimizes the fit between the simulated data and the measured data.

In this study, the network was conditioned by the different spread of radial basis functions' values and mean square error (MSE) as a performance goal. The spread of radial basis function value and the performance goal (MSE) value varied between 1 and 100 and 0 and 4 mm·d⁻¹, respectively. The optimum network structure was chosen by trial and error based on statistical indicators of test data.

2.4.2 Multi-layer perceptron

A multi-layer perceptron (MLP) is a feed-forward artificial neural network model that relates input data to adequate outputs. The MLP contains sets of multiple layers of neurons in directed graphs which are fully connected next to each other. It is an adjustment of the standard linear perceptron and can discern data that is not linearly separable (Cybenko 1989). The MLP architecture typically is defined by three layers, including input, hidden, and output layers (Fig. 3).

Formally, a one-hidden-layer MLP is a function $f: R^D \rightarrow R^L$, where D is the size of the input vector x and L is the size of the output vector $f(x)$, which is shown as follows:

$$f(x) = G\left(b^{(2)} + w^{(2)}\left(S\left(b^{(1)} + w^{(1)}x\right)\right)\right) \tag{5}$$

where $b^{(1)}$ & $b^{(2)}$ are the bias vectors, $w^{(1)}$ & $w^{(2)}$ are the weight matrices, and G and S are the transfer functions. The vector $U(x) = s(b^{(1)} + w^{(1)}x)$ organizes the hidden layer. $w^{(1)} \in R^{L \times M}$ is the weight matrix relating the input vector to the hidden layer with M neurons. Each column $w_i^{(1)}$ represents the weights from the input units to the i th hidden neuron. The common choices for S are tanh and sigmoid function. The output vector is acquired as: $f(x) = G(b^{(2)} + w^{(2)}(U(x)))$. $w^{(2)} \in R^{M \times D}$ is the weight matrix connecting the hidden layer to the output layer. The typical function for the output layer is linear.

For optimal training and simulation performance of ET_c, the model was evaluated with two hidden layers. The nodes of the first hidden layer vary from 4 to 15 and the second hidden layer varies from 5 to 30. Additionally, five transfer functions (hyperbolic tangent, log-sigmoid, hyperbolic tangent sigmoid, symmetric saturating linear, linear) for each layer, including the hidden layers and the output layer were tested. In this study, two learning algorithms, Levenberg–Marquardt and

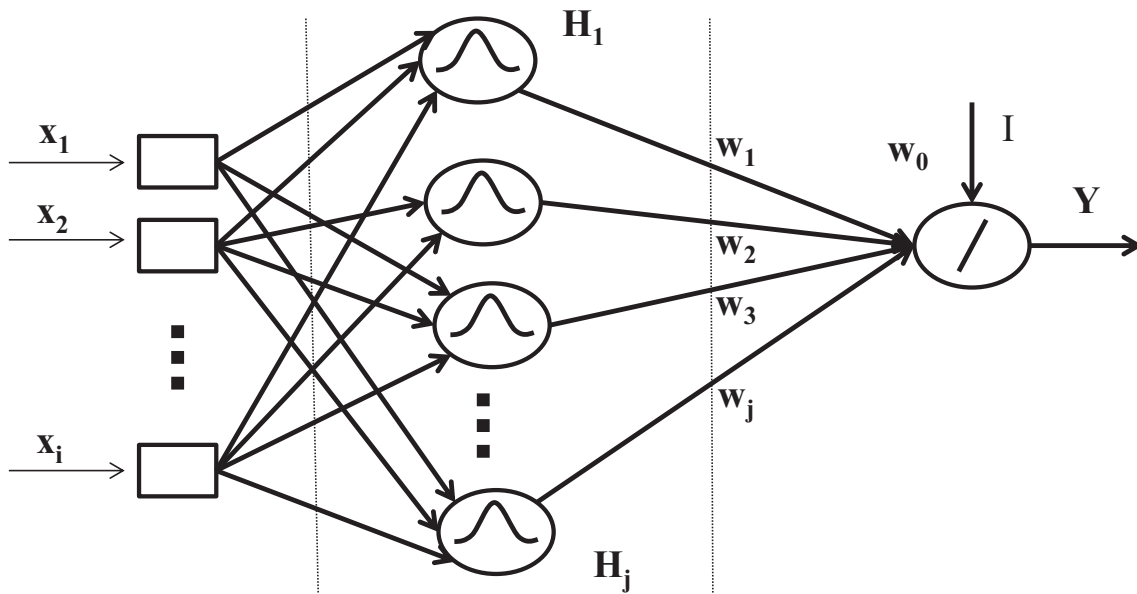


Fig. 2 Architecture of a radial basis function network

Bayesian regularization were assessed. The best function algorithm and the number of the nodes of the hidden layer were selected by a process of trial and error based on the statistical indicators.

these parameters have been calculated to determine the accuracy of the model as follows:

1. Normalized root mean square error (NRMSE):

2.5 Statistical analysis

Statistical analysis is an important tool to determine the accuracy of methods and select the best methods. In this work,

$$NRMSE = \sqrt{\frac{\sum_{i=1}^N (P_{obs} - P_{sim})^2}{NP_{obs}^2}} \tag{6}$$

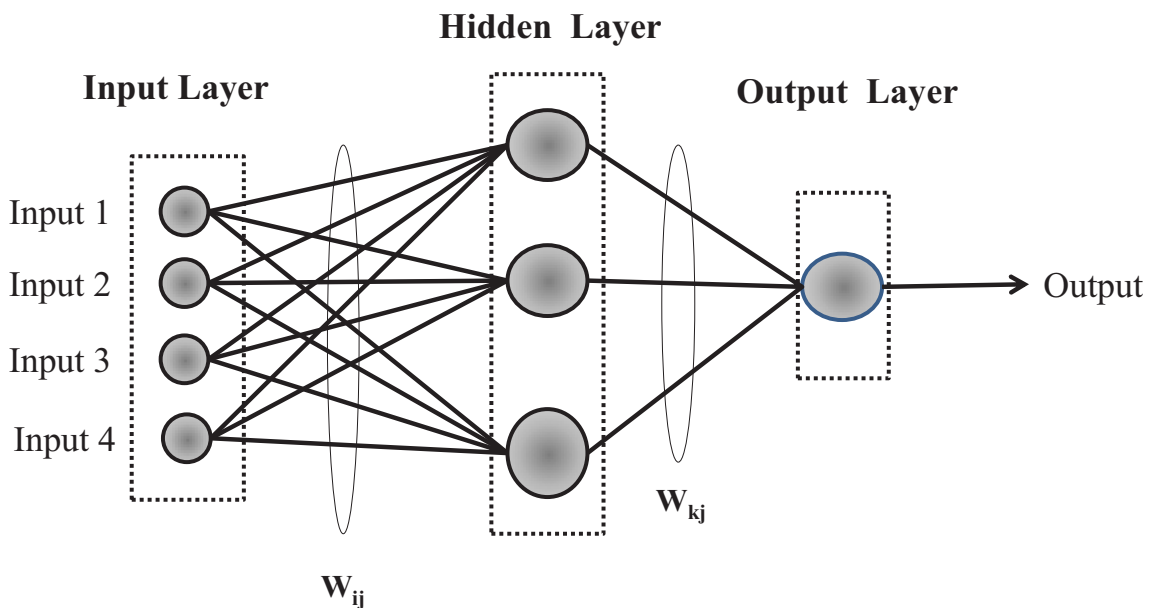


Fig. 3 Architecture of a multi-layer perceptron

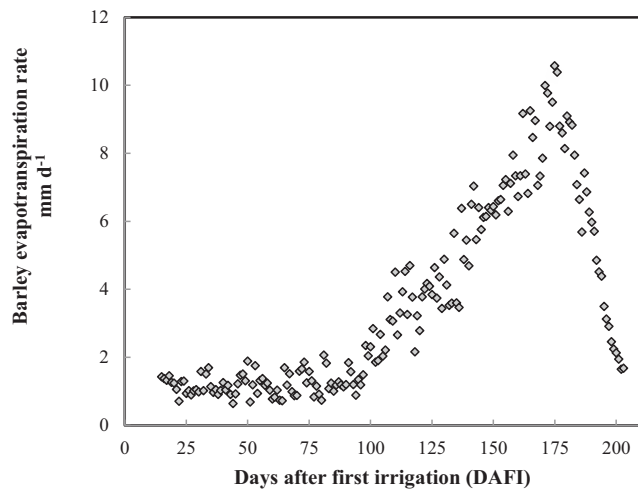


Fig. 4 Averages of measured DBSE from two lysimeters by days after first irrigation (DAFI)

where P_{sim} is the amount of simulated daily evapotranspiration, P_{obs} is the amount of observed daily evapotranspiration, and N is the number of observations. When the NRMSE is closer to zero, the high precision of the model in predicting ET_c is shown.

2. Mean Absolute Error (MAE):

$$MAE = \frac{\sum_{i=1}^N |(P_{obs} - P_{sim})|}{N} \tag{7}$$

When the value of this index is lower, it illustrates further precision of the model.

3. Index of agreement (d):

$$d = 1 - \frac{\sum_{i=1}^N (P_{sim} - P_{obs})^2}{\sum_{i=1}^N (|P_{sim} - \bar{P}_{obs}| + |P_{obs} - \bar{P}_{obs}|)^2} \tag{8}$$

where \bar{P}_{obs} is the mean amount of observed daily evapotranspiration. The index of agreement shows that the performance of the model is ideal (best) when the value is one or closer to one.

4. Mean bias error (MBE):

$$MBE = \frac{\sum_{i=1}^N (P_{sim} - P_{obs})}{N} \tag{9}$$

This index shows the mean overestimation and underestimation of the model. The lower the value of this index, the better the model.

5. R Square

$$R^2 = \frac{\sum_{i=1}^N (P_{sim} - \bar{P}_{sim})^2 (P_{obs} - \bar{P}_{obs})^2}{\sum_{i=1}^N (P_{sim} - \bar{P}_{sim})^2 \sum_{i=1}^N (P_{obs} - \bar{P}_{obs})^2} \tag{10}$$

R^2 is an index that indicates how well the data fit into a statistical model. The closer the index approaches one is better.

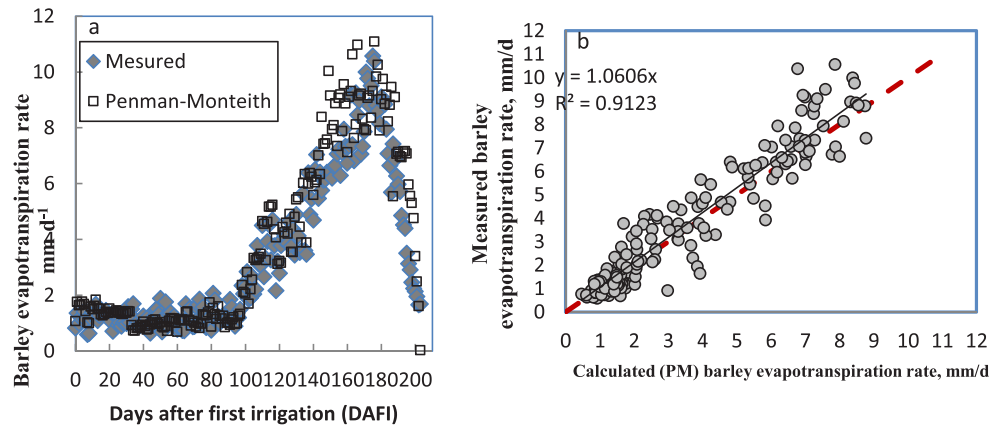
2.6 Sensitivity analysis for ANN

Sensitivity analysis is a prevailing approach for assessing the effect of each input data in the model on ET_c prediction. In general, artificial neural networks do not give information about the significant impact rate of input data on the output data. Process sensitive analysis specifies which input data has a higher effect and which has a lower effect; therefore, we can reduce the number of input data and develop a simpler model. Furthermore, we understand which data needs more precise measurement.

Table 1 Average barley evapotranspiration rate at different growth stages and its total seasonal measured and estimated by MLP-ANN, RBF-ANN, and Penman–Monteith

	Growth stages			
	Measured (mm day ⁻¹)	Penman–Monteith (mm day ⁻¹)	MLP-ANN (mm day ⁻¹)	RBF-ANN (mm day ⁻¹)
Initial stage	1.22	1.21	1.31	1.32
Developing stage	3.80	4.06	3.11	3.33
Mid stage	7.50	8.43	6.71	7.00
End stage	4.21	5.87	4.78	4.93
Total seasonal ET_c (mm)	689	783	654	680

Fig. 5 **a** The measured and estimated DBSE by Penman–Monteith by days after first irrigation (DAFI) and **b** linear regression between measured and calculated DBSE by PM method



In this study, sensitivity analysis was carried out by using dimensionless scaled sensitivity (DSS). This method demonstrates the sensitivity of the predicted parameters to the input data used. The dimensionless scaled sensitivity, SS_{ij} , is calculated as (Hill 1988):

$$SS_{ij} = \left(\frac{\partial y_i'}{\partial b_j} \right)^{w_i} b_j \tag{11}$$

where j represents one of the inputs, i represents one of the observations, y_i' is the predicted value associated with the i th observation, b_j is the j th computed input, $\frac{\partial y_i'}{\partial b_j}$ is the sensitivity of the simulated value associated with the i th observation according to the j th input and is assessed at the final input value and w_i is the weight of the i th observation (in this search it is equal to one for every observation). ∂b_j is the amount of change to the inputs and ∂y_j is the amount of change predicted for the value associated with the i th observation.

Composite scaled sensitivities (CSS) are computed for each input using the scaled sensitivities for all observations. They are dimensionless, so can be used to evaluate the amount of CSS with different types of inputs. Model simulation results are more sensitive to inputs that have a large CSS. The CSS

for j th input is computed as (Hill 1988):

$$CSS_j = \left[\frac{\sum_{i=1}^N (SS_{ij})^2}{N} \right]^{0.5} \tag{12}$$

where N is the number of observations, SS_{ij} is the scaled sensitivities, i is the observed value, and j is the number of input data.

For this purpose, the sensitivity analysis was carried out in three steps:

1. Each state was generated by changing each input within a range of -20 to $+20\%$ at an interval of $\pm 5\%$ while keeping other parameters constant.
2. The change of ET_c for each state was predicted using the optimum networks.
3. The scaled sensitivities (SS_{ij}) for each observation and the Composite Scaled Sensitivities (CSS_j) were computed for each state.

3 Results and discussion

The DBSE was determined based on the principle of soil water balance in the weighing lysimeter and the average of measured DBSE in two lysimeters was considered as the daily barley standard evapotranspiration. The DBSE as a function of days after first irrigation (DAFI) was shown in Fig. 4.

The value of barley ET_c during the growing season, between the emergence and stem elongation, is very low due to low LAI, temperature, and winter frost conditions. The mean daily average ET_c was only about 1.1 mm day^{-1} at the early growth stage and increased as both temperature and canopy growth increased. The DBSE increased rapidly, until to the end of the mid-season stage. The maximum DBSE rate occurred at 172–183 DAFI, with a mean value of 9.5 mm day^{-1} . Total measured crop ET_c was 689 mm.

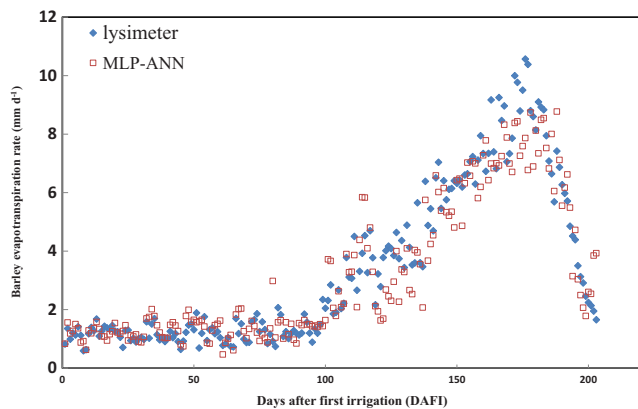
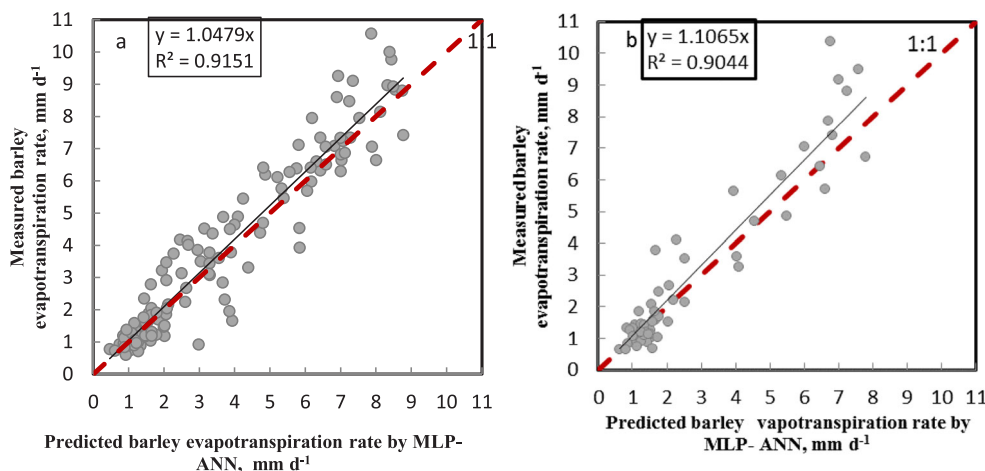


Fig. 6 Comparison between the measured and estimated DBSE by MLP-ANN

Fig. 7 Linear regression between the measured and predicted DBSE for **a** training set and **b** testing set



3.1 Penman–Monteith ET_c

Daily barley ET_c was estimated using the Penman–Monteith equation. The average calculated ET_c rate in individual growth stage was shown in Table 1. The results indicated that for each growth stage except the initial stage, the mean calculated ET_c rate was higher than the measured values and total calculated seasonal ET_c was 13% higher than the measured seasonal ET_c . Figure 5 a, b show the comparison between the measured and estimated DBSE. The measured values of DBSE and the calculated Penman–Monteith ET_c in Fig. 5a followed the same pattern. From day 1 to day 30, the DBSE rate was very low at least as $2.0 \text{ mm}\cdot\text{d}^{-1}$. After day 100, the rate increased gradually from 2.0 to $10.0 \text{ mm}\cdot\text{d}^{-1}$ until day 170. The Penman–Monteith ET_c showed a higher DBSE rate of about $11.0 \text{ mm}\cdot\text{d}^{-1}$ when as compared with the measured values which had lower rates of about $10.0 \text{ mm}\cdot\text{d}^{-1}$. The difference was about 10%.

The linear relationship between the predicted amount of DBSE by Penman–Monteith and the measured value has been plotted and compared with 1:1 line in Fig. 5b.

The value of the intercept was not significantly different than zero. Therefore, a linear regression without intercept was

fitted to the data. The equation of linear regression is shown below:

$$ET_{c\text{Measured}} = 1.06 \times ET_{c\text{Simulated}} \tag{13}$$

3.2 ET_c by the ANN methods

3.2.1 Result of multi-layer perceptron artificial neural network

The training and testing results showed that multi-layer perceptron artificial neural network’s structures with two hidden layers and its structure 4-8-5-1, and Levenberg–Marquardt learning algorithm and hyperbolic tangent transfer function for hidden layers and linear transfer function for output layer had the best prediction. Moreover, with linear regression, the relationship between the predicted DBSE by neural network and the measured value has been plotted. The plotted line has been compared with the 1:1 line. The difference between the obtained slope and intercept of the linear regression equation with 1.0 and 0 was not statistically significant at the 5% level of probability. Therefore, the relationship between the simulated DBSE by MLP-ANN and the measured values has been computed with a linear regression model without intercept for the testing and training data. Results have been shown in Figs. 6 and 7. The equations of the linear regression are as follows:

$$\text{Training : } ET_{c\text{Measured}} = 1.047 \times ET_{c\text{Simulated}} \tag{14}$$

$$\text{Testing : } ET_{c\text{Measured}} = 1.106 \times ET_{c\text{Simulated}} \tag{15}$$

Figure 6 indicated that the measured and simulated DBSE followed the same pattern with different rates. The MLP-ANN estimated the DBSE of the end season average rate which was lower than the measured values, and in the remaining seasons, the simulated values were closer to the measured values

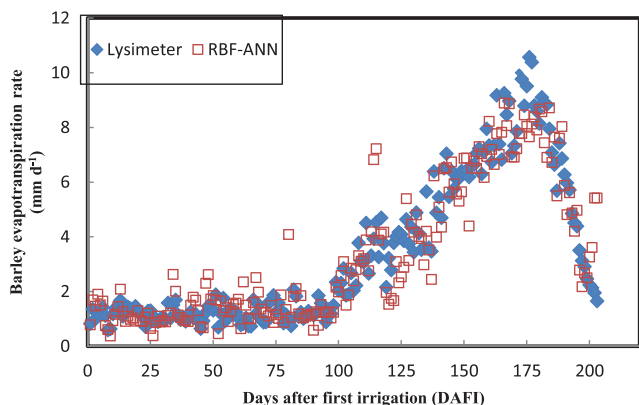
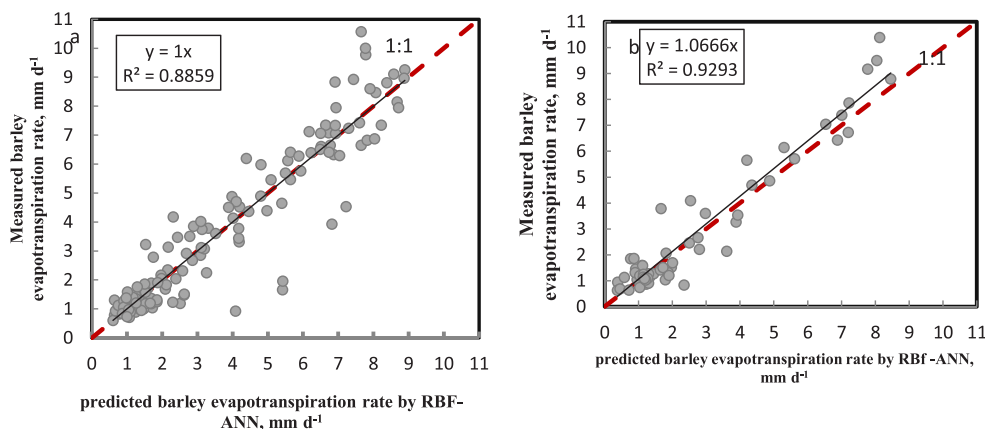


Fig. 8 Comparison between the measured and estimated DBSE by RBF-ANN

Fig. 9 Linear regression between the measured and predicted DBSE for a training set and b testing set



(Table 1). In general, the results showed seasonal ET_c was computed at 5% lower than the measured value by the MLP-ANN.

$$\text{Training : } ET_{c\text{Measured}} = 1.0 \times ET_{c\text{Simulated}} \tag{16}$$

$$\text{Testing : } ET_{c\text{Measured}} = 1.066 \times ET_{c\text{Simulated}} \tag{17}$$

3.2.2 Result of radial basis function artificial neural network

The result (Figure 8) showed that the network had the best performance with a spread of radial function value of 39 and mean square error of 0.5. A linear regression model has been fitted to the relationship between the simulated amounts of barley evapotranspiration by the neural network (RBF-ANN) and the measured values (Fig. 9a, b).

This linear regression has been compared with a 1:1 line, and the comparison between the fitted line and 1:1 line at 5% level of probability has been investigated. The results showed that the difference between the regression slope and intercept, respectively, with 1.0 and 0.0 at the chosen level of probability (5%), was not statistically significant (Fig. 9a, b). Finally, the relationship between the simulated DBSE by RBF-ANN and the measured values with a linear regression model without intercept has been fitted for testing and training data in (Fig. 9a, b). The equations of linear regression without intercept of data are as follows:

Figure 8 showed that the measured and simulated DBSE follow the same pattern. The RBF-ANN simulated the mean barley ET_c rate in each growth stage of crop closer to the measured values (Table 1). Furthermore, the seasonal ET_c was estimated about 1.3% lower than the measured value by The RBF-ANN.

The statistical indices were computed for indirect methods (MLP-ANN, RBF-ANN, and Penman–Monteith) for estimating the DBSE in a semi-arid region (Table 2). Results indicated that the three methods have acceptable performance according to each statistical index (Table 2).

3.3 Sensitivity analysis

Figure 10a showed the results of the sensitivity analysis of barley ET_c obtained by MLP-ANN model for each of the weather parameters. The most sensitive variable for ET_c was

Fig. 10 The dimensionless composite scaled sensitivities of DBSE with response to change in climate variable in **a** MLP-ANN model and **b** RBF-ANN model

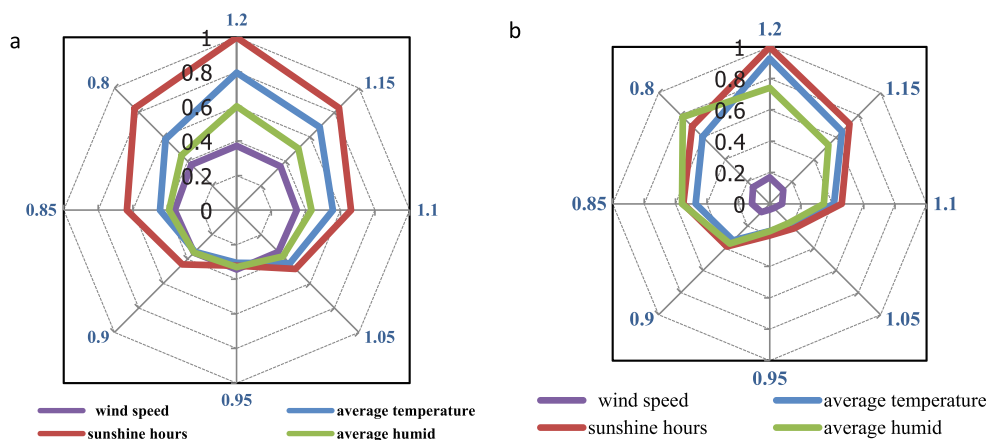


Table 2 Statistical indicators of DBSE estimated by MLP-ANN, RBF-ANN, and Penman–Monteith

Statistical parameters	MLP-ANN		RBF-ANN		Penman–Monteith
	Test	Training	Test	Training	
R^2	0.91	0.92	0.93	0.89	0.92
MBE	– 0.20	– 0.16	– 0.15	0.00	0.46
NRMSE	0.31	0.23	0.26	0.25	0.30
MAE	0.58	0.58	0.52	0.60	0.71
D	0.99	0.97	0.87	0.82	0.79

the sunshine hours (Rn) and the wind speed was the least. In response to the increase in Rn by + 20%, the percent change in seasonal ET_c was about 7%. A 20% increase in the wind speed caused the seasonal ET_c to increase by about 3%. The dimensionless composite scaled sensitivities showed that the barley ET_c was less effective in the range of change in the value of all variables from – 10 to 5%.

Figure 10b indicated the results of the sensitivity analysis of barley ET_c obtained by RBF-ANN model for each of the inputs. In this model, the curves showed a different pattern compared with MLP-ANN. The most sensitive variable for ET_c was the sunshine hours (Rn) followed closely by decreasing values of variables by higher than 10%. When the average humidity was decreased higher than 10%, it becomes the most sensitive variable. The wind speed was the least sensitive variable for ET_c in all levels of changes. In response to the increase in Rn by + 20%, the percent change in seasonal ET_c was about 7% and a 20% increase in wind speed caused the seasonal ET_c to increase by about 3%. The ET_c showed less change by the dimensionless composite scaled sensitivity analysis in the range of change values for all variables from – 10 to 10%.

4 Conclusions

The barley standard ET_c was measured by two weighing lysimeters in a semi-arid region. The highest barley ET_c occurred between 172–183 DAFI, with an average of 9.5 mm day⁻¹ and the seasonal ET_c of 689 mm. This information would be used by stockholders to optimize cropping pattern based on the supply of water resources as well as managing deficit irrigation.

In this study, the potential of the artificial neural network with two kinds of the multi-layer perceptron and the radial basic function and Penman–Monteith models for estimating DBSE using climatological data have been investigated. Although all approaches have acceptable accuracy, the ANNs is more applicable due to its need for fewer variables.

Results of sensitivity analysis showed that in the multi-layer perceptron, barley ET_c was more sensitive to sunshine

hours and less sensitive to wind speed and the radial basic function was more sensitive to sunshine hours (Rn). In contrast, when Rn was decreased more than 10%, ET_c was more sensitive to average humidity.

It was found that Rn was an important factor in input data of networks for estimating barley ET_c ; therefore, it was very important for decision making to find the best methods and technologies to improve the estimation of ET_c .

Funding information This research was supported in part by a research project funded by grant no. 98-GR-AGR 42 of Shiraz University Research Council, Drought National Research Institute, the Center of Excellence for On-Farm Water Management, and Iran National Science Foundation (INSF).

References

- Abrishami N, Sepaskhah AR, Shahrokhnia MH (2019) Estimating wheat and maize daily evapotranspiration using artificial neural network. *Theor Appl Climatol* 135(3-4):945–958
- Aghajanjoo MB, Sabziparvar AA, Hosseinzadeh-Talaei P (2012) Artificial neural network–genetic algorithm for estimation of crop evapotranspiration in a semi-arid region of Iran. *Neural Comput & Applic* 23:1387–1393. <https://doi.org/10.1007/s00521-012-1087-y>
- Allen RG, Pereira LS, Raes D, Smith M (1998) Crop evapotranspiration—guidelines for computing crop water requirements. FAO Irrigation and Drainage Paper 56, vol 300. FAO, Rome, p 654
- Ambas VT, Baltas E (2012) Sensitivity analysis of different evapotranspiration methods using a new sensitivity coefficient. *Global NEST* 14(3):335–343
- Beven K (1979) A sensitivity analysis of the Penman-Monteith actual evapotranspiration estimates. *J Hydrol* 44:169–190
- Cybenko G (1989) Approximation by superpositions of a sigmoidal function. *Math Control Signals Syst* 2:303–314
- Dehbozorgi F, Sepaskhah AR (2012) Comparison of artificial neural networks and prediction models for reference evapotranspiration estimation in a semi-arid region. *Arch Agron Soil Sci* 58(5):477–497
- Falamarzi Y, Palizdan N, Huang YF, Lee TS (2014) Estimating evapotranspiration from temperature and wind speed data using artificial and wavelet neural networks (WNNs). *Agric Water Manag* 140:26–36
- Gong L, Xu CY, Chen D, Halldin S, Chen YD (2006) Sensitivity of the Penman-Monteith reference evapotranspiration to key climate variable in the Changjiang (Yangtze river) basin. *J Hydrol* 329:620–629

- Hashemi M (2013) Determination of crop coefficients and potential evapotranspiration for barley by weighing lysimeter in Kooshkak region, Fars province. M.S. thesis. Shiraz University.(in Persian).
- Hill MC (1988) Methods and guidelines for effective model calibration: US Geological Survey water resource investigations Report 98-4005. 90p
- Kisi Ö (2010) Evapotranspiration modeling using a wavelet regression model. *Irrig Sci* 29:241–252
- Kisi O, Kilic Y (2015) An investigation on generalization ability of artificial neural networks and M5 model tree in modeling reference evapotranspiration. *Theor Appl Clim* 126:413–425. <https://doi.org/10.1007/s00704-015-1582-z>
- Kumar M, Bandyopadhyay A, Raghuvanshi NS, Singh R (2008) Comparative study of conventional and artificial neural network-based ETo estimation models. *Irrig Sci* 26:531–545
- Kumar M, Raghuvanshi NS, Singh R (2011) Artificial neural networks approach in evapotranspiration modeling: a review. *Irrig Sci* 29:11–25. <https://doi.org/10.1007/s00271-010-0230-8>
- Ladlani I, Houichi L, Djemili L, Heddami S, Belouz K (2012) Modeling daily reference evapotranspiration (ET₀) in the north of Algeria using generalised regression neural networks (GRNN) and radial basis function neural networks (RBFNN): a comparative study. *Meteorol Atmos Phys* 118:163–178
- Landeras G, Ortiz-Barredo A, Lopez JJ (2008) Comparison of artificial neural network models and empirical and semi-empirical equations for daily reference evapotranspiration estimation in the Basque Country (Northern Spain). *Agric Water Manag* 95:553–565
- Li YL, Cui JY, Zhang TH, Zhao HL (2003) Measurement of evapotranspiration of irrigated spring wheat and maize in a semi-arid region of north China. *Agric Water Manag* 61:1–12
- Malek E 1982 Methods of evaluating water balance and determining climate type: an example for Bajgah, Iran. *Iran J Agri Sci* 12:57–72 (in Persian)
- Moghaddamnia A, Ghafari Gousheh MG, Piri J, Amin S, Han D (2009) Evaporation estimation using artificial neural networks and adaptive neuro-fuzzy inference system techniques. *Adv Water Resour* 32:88–97
- Saltelli A, Tarantola S, Campolongo F, Ratto M (2004) Sensitivity analysis in practice. Wiley. 232P
- Shahrokhnia MH, Sepaskhah AR (2012) Evaluation of wheat and maize evapotranspiration determination by direct use of the Penman-Monteith equation in a semi-arid region. *Arch Agron Soil Sci* 58:1283–1302
- Shahrokhnia MH, Sepaskhah AR (2013) Single and dual crop coefficients and crop evapotranspiration for wheat and maize in a semi-arid region. *Theor Appl Clim* 114:495–510
- Sharifi A, Dinpazhoh Y (2014) Sensitivity analysis of the Penman-Monteith reference crop evapotranspiration to climatic variables in Iran. *Water Resour Manag* 28:5465–5476
- Sudheer KP, Gosain AK, Ramasastri KS (2003) Estimating actual evapotranspiration from limited climatic data using neural computing technique. *J Irrig Drain Eng* 129(3):214–218
- Trajkovic S (2005) Temperature-based approaches for estimating reference evapotranspiration. *J Irrig Drain Eng* 131:316–323
- Traore S, Wang Y, Kerh T (2010) Artificial neural network for modeling reference evapotranspiration complex process in Sudano-Sahelian Zone. *Agric Water Manag* 97:707–714
- Zanetti SS, Sousa EF, Oliveira VP, Almeida FT, Bernardo S (2007) Estimating evapotranspiration using artificial neural network and minimum climatological data. *J Irrig Drain Eng* 133:83–89. <https://doi.org/10.1061/ASCE0733-9437>

Publisher's note Springer Nature remains neutral with regard to jurisdictional claims in published maps and institutional affiliations.